ANTIOXIDANTS & REDOX SIGNALING
Volume 16, Number 10, 2012

DOI: 10.1089/ars.2011.3960

ORIGINAL RESEARCH COMMUNICATION

NADPH Oxidase 1-Mediated Oxidative Stress Leads to Dopamine Neuron Death in Parkinson's Disease

Dong-Hee Choi,[1,2] Ana Clara Cristóvão,[1,3,4] Subhrangshu Guhathakurta,[1,3] Jongmin Lee,[5] Tong H. Joh,[1] M. Flint Beal,[1] and Yoon-Seong Kim[1,3,6]

Abstract

Aim: Oxidative stress has long been considered as a major contributing factor in the pathogenesis of Parkinson's disease. However, molecular sources for reactive oxygen species in Parkinson's disease have not been clearly elucidated. Herein, we sought to investigate whether a superoxide-producing NADPH oxidases (NOXs) are implicated in oxidative stress-mediated dopaminergic neuronal degeneration. ***Results:*** Expression of various Nox isoforms and cytoplasmic components were investigated in N27, rat dopaminergic cells. While most of Nox isoforms were constitutively expressed, Nox1 expression was significantly increased after treatment with 6-hydroxydopamine. Rac1, a key regulator in the Nox1 system, was also activated. Striatal injection of 6-hydroxydopamine increased Nox1 expression in dopaminergic neurons in the rat substantia nigra. Interestingly, it was localized into the nucleus, and immunostaining for DNA oxidative stress marker, 8-oxo-dG, was increased. Nox1expression was also found in the nucleus of dopaminergic neurons in the substantia nigra of Parkinson's disease patients. Adeno-associated virus-mediated Nox1 knockdown or Rac1 inhibition reduced 6-hydroxydopamine-induced oxidative DNA damage and dopaminergic neuronal degeneration significantly. ***Innovation:*** Nox1/Rac1 could serve as a potential therapeutic target for Parkinson's disease. ***Conclusion:*** We provide evidence that dopaminergic neurons are equipped with the Nox1/Rac1 superoxide-generating system. Stress-induced Nox1/Rac1 activation causes oxidative DNA damage and neurodegeneration. Reduced dopaminergic neuronal death achieved by targeting Nox1/Rac1, emphasizes the impact of oxidative stress caused by this system on the pathogenesis and therapy in Parkinson's disease. *Antioxid. Redox Signal.* 16, 1033–1045.

Introduction

Oxidative damage to specific neurons in the central nervous system (CNS) is a commonly observed pathophysiologic feature of neurodegenerative diseases such as Parkinson's disease (PD) and Alzheimer's disease (AD). A wide range of oxidative damage to cellular macromolecules in nigrostriatal dopaminergic neurons, including lipids, proteins, and nucleotides, has been observed in postmortem brains of PD patients. The molecular mechanism underlying selective susceptibility of the nigrostriatal pathway to oxidative stress remains unresolved. Mitochondrial dysfunctions, including selective decrease in respiratory complex I activity and mitochondrial DNA abnormality (7, 40), are implicated in

Innovation

In the present study, we have demonstrated that Nox1/Rac1 is activated in dopaminergic neurons under stress conditions, causing oxidative stress and consequential neuronal death. Nuclear localization of Nox1and oxidative DNA damage were observed in both rodent PD model and postmortem human PD brain tissue. AAV-mediated targeting against Nox1/Rac1 protects dopaminergic neurons under 6-OHDA toxicity, proposing Nox1 and Rac1 as novel molecular targets for therapeutic intervention in PD.

[1]Neurology/Neuroscience Department, Weill Medical College of Cornell University, New York, New York.
Departments of [2]Medical Science and [5]Rehabilitation Medicine, Graduate School of Medicine, Konkuk University, Seoul, South Korea.
[3]Burnett School of Biomedical Sciences, College of Medicine, University of Central Florida, Orlando, Florida.
[4]Ph.D. Program in Experimental Biology and Biomedicine, Center for Neuroscience and Cell Biology, University of Coimbra, Coimbra, Portugal.
[6]College of Nursing Science, Kyunghee University, Seoul, South Korea.

the pathogenesis of PD partly through an increase in the production of the reactive oxygen species (ROS). Moreover, a significant increase in oxidative damage to DNA in both nucleus and mitochondria has been observed in dopaminergic neurons in the substantia nigra (SN) of PD patients (2, 31, 41). However, the mechanisms of DNA damage, especially nuclear DNA damage, are obscure.

Increasing evidence has suggested that the family of NADPH oxidases (NOX), the enzyme complex that transports electrons across the plasma membrane and generates superoxide, plays a major role in generating ROS in cells (5). NOX was first discovered in neutrophils (39), and seven homologues including NOX1, NOX2, NOX3, NOX4, NOX5, DUOX1, and DUOX2 have been identified in various tissues (11, 15, 17, 45). ROS at moderate concentrations are necessary for biological processes such as development, memory, neuronal signaling, and cardiovascular homeostasis. However, ROS at higher concentrations in cells have deleterious effects on cellular homeodynamics that include damage to cellular components, such as DNA in both nucleus and mitochondria. Nox is a dedicated superoxide generating enzyme complex and probably a candidate for the production of high concentrations of ROS. Nox homologues are found in the CNS (43), and are linked to pathologic conditions of the same (6, 29, 50). Nox1 is the inducible enzyme in the family and Rac1 is an essential subunit for the activation of Nox1.

We have previously shown that Nox1 expression is increased in dopaminergic neurons in the SN of mice in response to an environmental toxin, paraquat, and that it was responsible for neurodegeneration (13). Since paraquat induces selective degeneration of SN dopaminergic neurons, it is used to generate a rat model of PD, accumulation of Nox1 in SN dopaminergic neurons of paraquat-treated rats may imply that it happens in the brain of idiopathic PD patients. Lines of evidence suggest that there is cross talk between mitochondria and transcriptional activation of Nox1 (14, 25, 28), and a role of mitochondria in neurodegeneration has to be considered along with Nox1 expression in neurons. Of particular interest, the finding that Nox isoforms localize to specific subcellular organelles, including mitochondria and the nucleus (10, 16, 27), may cause ROS accumulation and damage to their contents such as DNA.

We developed the adeno-associated virus serotype 2 (AAV2)-mediated overexpression or knockdown system and established an effective method for the genetic intervention of Nox1 and Rac1, specifically in SN dopaminergic neurons *in vivo*. Hereby we present the critical evidence that accumulation of the Nox1/Rac1 complex and ROS in the nucleus of SN dopaminergic neurons is directly responsible for nuclear DNA damage which leads to dopaminergic neurodegeneration. Also the genetic intervention to Nox1 and Rac1 and the chemical inhibition of Nox1, protect nuclear DNA from damage and thus are neuroprotective.

Results

Nox1 induction and activation of the NADPH oxidase system in dopaminergic cells

The NADPH oxidase is a multi-subunit enzyme that consists of the catalytic subunits(Nox isoforms) together with the regulatory subunits including p22phox, p47phox, p40phox, p67phox, Nox organizer 1 (Noxo1), Nox activator 1 (Noxa1), and small GTPase Rac1. In order to test whether dopaminergic (DA) cells are equipped with the NOX components, N27, a well-established rat DA cell line was examined (35). The mRNAs encoding each Nox isoform and regulatory subunits were detected using RT-PCR. Since transcriptional induction of Nox1 and Nox4 has already been reported in several tissues under a variety of stimuli, transcripts were determined in both nontreated and 6-hydroxydopamine (6-OHDA), a DA neurodegenerative compound, treated DA cells. ROS generation as induced by 6-OHDA (100 μM) and subsequent cell death was observed (Supplementary Figs. 1 A and 1B; Supplementary data are available online at www.liebertonine.com/ars). All Nox isoforms (Nox1, Nox2, Nox4, Duox1 and Duox2) except Nox3 and Nox5 were detected (Fig. 1A). While other variants were expressed constitutively, Nox1 was robustly induced by 100 μM 6-OHDA treatment for 6 h (Fig. 1A). Mitochondria, which have long been considered as a major source of ROS, play a key role in Nox1-mediated superoxide generation (16, 28, 48). Mitochondrial respiratory complex inhibitors which increased mitochondrial ROS (Supplementary Fig. 2C) also induced Nox1 (Supplementary Figs. 2A and 2B) in N27 cells, suggesting a role of mitochondrial ROS in Nox1 induction. Cytoplasmic regulatory subunits including p47phox, Noxa1, and Noxo1 were constitutively expressed in DA cells as well (Fig. 1A). Noxa1 and Noxo1 are homologues of p67phox and p47phox, respectively. They are involved in Nox1-mediated superoxide generation (4, 20). Treatment with 6-OHDA induced Nox1 expression in a dose-dependent manner as shown by the immunoblot analysis (Fig. 1B). The activation of a small GTPase Rac1 is indispensable for Nox1 and Nox2 activation (9). GTP-bound active Rac1 was measured in DA cells treated with 6-OHDA for various duration from 1 h to 6 h. Rac1 activation was observed at 6 h post 6-OHDA administration and Nox1 was co-precipitated with active Rac1 (Fig. 1C).

The NADPH oxidase system plays a pivotal role in 6-OHDA-mediated ROS generation

To evaluate whether NADPH oxidase system is responsible for 6-OHDA-induced superoxide generation, two widely used chemical inhibitors, diphenyleneiodonium (DPI) and apocynin were tested. N27 cells were pre-treated with various concentrations of DPI (0.1, 0.5, and 1.0 μM) for 30 min and then 6-OHDA (100 μM) was added. Superoxide was measured using the nitroblue tetrazolium (NBT) assay at 6 h post 6-OHDA. DPI significantly reduced 6-OHDA-mediated ROS generation at concentration as low as 0.1 μM (Figs. 2A and 2B). Due to the nonspecific inhibitory action of DPI on other flavin-dependent enzymes, apocynin, a potent intracellular inhibitor of the assembly of NADPH oxidase, was tested (44). Pretreatment of DA cells for 30 min with various concentrations of apocynin (0.1, 1.0, 10, 100 μM) also significantly diminished ROS production by 6-OHDA (Figs. 2C and 2D). To selectively inhibit Nox1, Nox1 knockdown was achieved by RNAi. Nox1 knockdown efficiency of siRNA nucleotide sequence was assessed by both RT-PCR and immunoblotting at 36 h post transfection (Fig. 2E). Transfection efficiency of siRNA nucleotide sequence into N27 cells was tested using fluorescent-tagged siRNA, showing about 37% fluorescence positive cells after 36 h post transfection (Supplementary Fig. 3). In parallel with the transfection rate, 6-OHDA-mediated ROS generation was decreased (Fig. 2F).

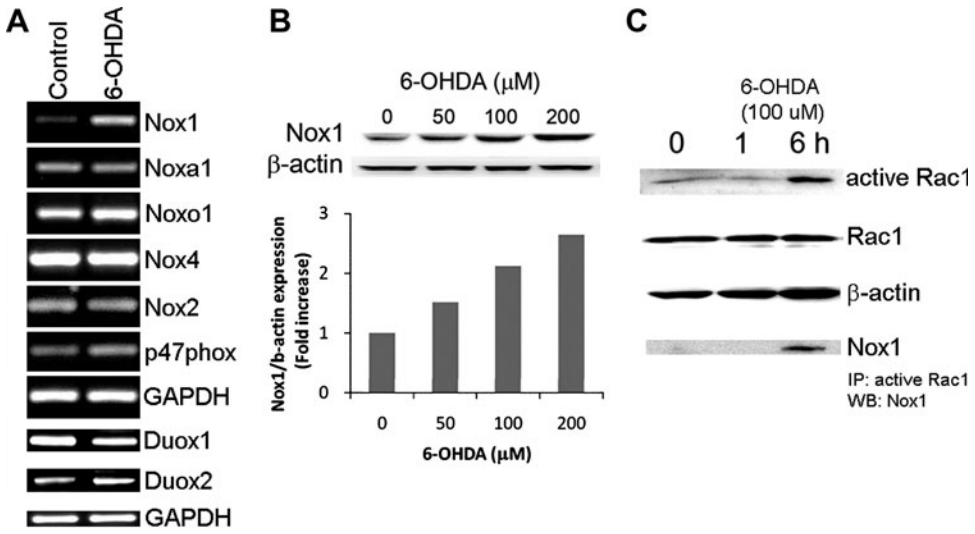

FIG. 1. Dopaminergic cells contain NADPH oxidase components and 6-OHDA leads to Nox1induction and Rac1 activation. (A) mRNA of Nox isoforms and subunits were detected using RT-PCR in N27 cells treated with 6-OHDA (100 μM) for 6 h. GAPDH, internal control; control, vehicle treated. **(B)** 24 h 6-OHDA treatment increased Nox1 expression in a dose-dependent manner as examined by immunoblot analysis. Signal intensity was measured by Quantity One software and shown as a fold increase. β-actin, internal control. **(C)** GTP-bound active Rac1 was increased by 6-OHDA treatment for various durations (1 h and 6 h) as determined by the active GTPase pull-down assay. Nox1, coprecipitated with active Rac1, was detected in the same blot using Western blot analysis. Total Rac1 and β-actin were demonstrated as internal controls. Images are representative of three independent experiments.

Expression of Nox1 in nigrostriatal DA neurons of PD animal model

The observation that Nox1 was induced by a variety of oxidative stimuli *in vitro* led us to test Nox1 expression in the rat substantia nigra DA (SNDA) neurons administered with 6-OHDA. In comparison to vehicle treatment, a significant increase of Nox1 expression was observed in the substantia nigra (SN) after 3 days of 6-OHDA striatal injection (Fig. 3A). Neurons immunostained for Nox1 (red) displayed coexpression of tyrosine hydroxylase (TH) (green) in the SN, indicating DA neuron-specific expression of Nox1 (Fig. 3A). Neither astrocytes nor microglia expressed Nox1, as verified by co-immunostaining of Nox1 with GFAP (astrocytes) or CD11b (microglia) (Fig. 3B). Increased Nox1 transcript was found in the SN as shown by *in situ* hybridization (Fig. 3C). Increased Nox1 expression in the SNDA neurons was also observed in mice treated with 1-methyl-4-phenyl-1,2,3,6 -tetrahydropyridine (MPTP), a specific DA neurotoxin (Supplementary Fig. 4). Confocal microscopic analysis showed that constitutively expressed low-level Nox1 in the nucleus of DA neurons was significantly increased by 6-OHDA administration. As early as 3 days post 6-OHDA injection, Nox1 expression was increased in the nucleus and in the cytoplasm of DA neurons (Fig. 4A). About 75% of TH-positive neurons also showed Nox1 nuclear staining after 6-OHDA administration. Nuclear expression of the Nox1/Rac1 complex was further analyzed in N27 cells after treatment with 6-OHDA. First, activated Rac1 was detected by immunoprecipitation of nuclear extracts of N27 cells after a 24 h treatment with 6-OHDA. Increased Nox1 was also observed in the same blot, suggesting that Nox1 in the nucleus forms an active complex with GTP-bound Rac1 (Figs. 4B and 4C). Next, we established N27 cells stably expressing Nox1 tagged with EGFP at the C-terminus. Six h 6-OHDA treatment resulted in the translocation of Nox1-EGFP into the nucleus (Fig. 4D). To examine whether nuclear translocation of Nox1in dopaminergic cells is observed under different conditions that cause dopaminergic neuronal death, mitochondrial respiratory complex inhibitor, rotenone, was tested. Rotenone also led to nuclear localization of Nox1 (Fig. 4E). The presence of Nox1 in the nucleus of TH-positive DA neurons in the SN of postmortem brains of PD patients was observed in four PD subjects and none of controls (Fig. 4E), further supporting our hypothesis that Nox1 plays a role in degeneration of DA neurons in PD. Our results demonstrate for the first time that an active Nox1/Rac1 complex is formed in the nucleus of oxidatively stressed DA neurons.

Nuclear Nox1/Rac1 caused DNA oxidative damage in DA cells

To substantiate that nuclear Nox1/Rac1 complex produces superoxide, we investigated whether selective inhibition of the Nox1/Rac1 complex attenuates ROS production. Adeno-associated virus serotype 2 (AAV2) expression cassettes with either Nox1shRNA (Supplementary Figs. 5A and B) or a T17N dominant negative Rac1 variant were used to knockdown Nox1 or inhibit Rac1, respectively. These vectors separately expressed Green Fluorescent Protein (GFP) as a marker for transduction efficiency. Nox1 knockdown by Nox1shRNA (Fig. 5A) or Rac1 inhibition by T17NRac1 (Fig. 5B) significantly reduced 6-OHDA-mediated ROS generation in N27 cells. The increased levels of active Nox1/Rac1 complex (Fig. 4B) in the nucleus, and increased ROS (Figs. 5A and 5B) of DA cells in the presence of 6-OHDA, led us to investigate whether oxidative DNA damage occurs in the nucleus. In fact, 6-OHDA treatment increased DNA oxidative damage as determined by increased 8-oxo-dG immunoreactivity in the nucleus of both N27 cells and DA neurons in the rat SN

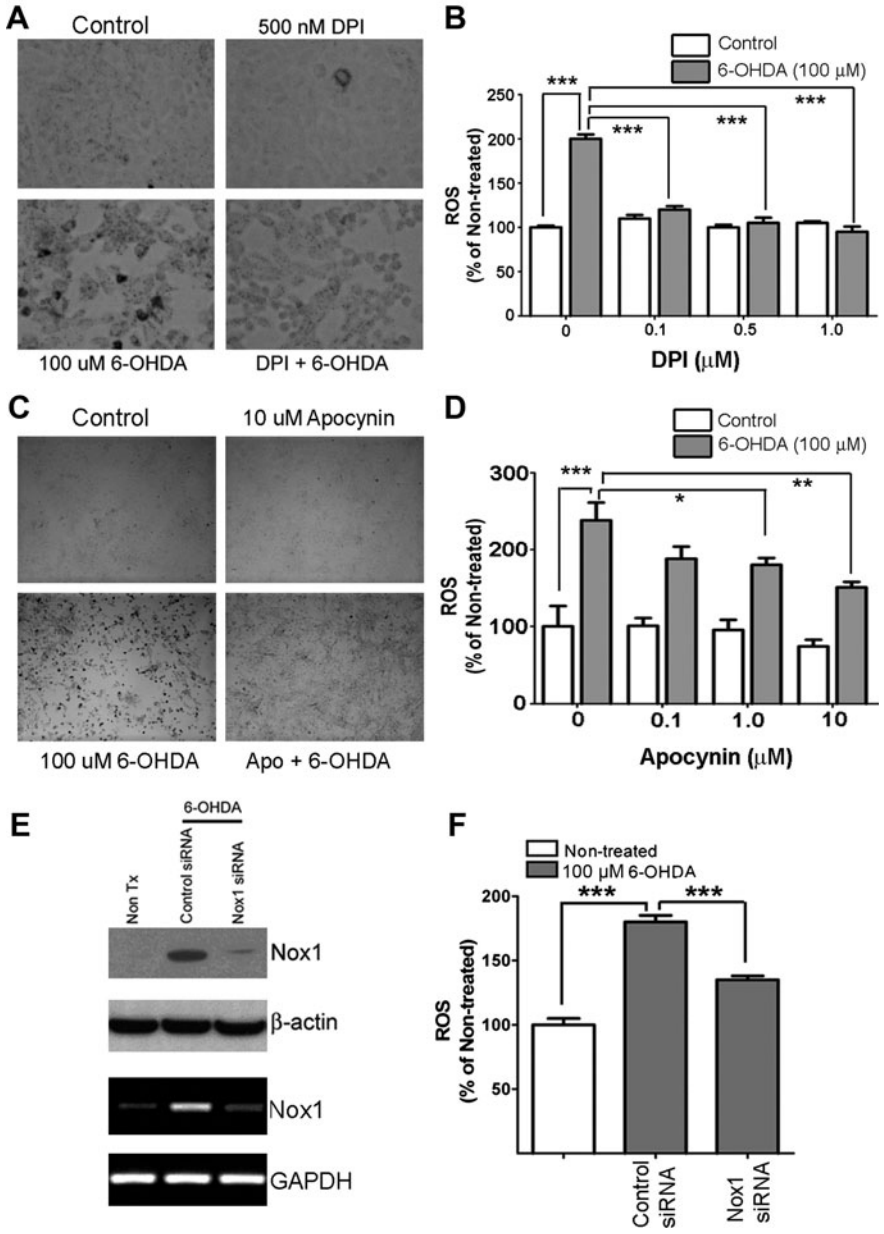

FIG. 2. NADPH oxidase is responsible for 6-OHDA-mediated ROS generation in dopaminergic cells. (A and **B)** ROS generation was measured using the NBT staining in N27 dopaminergic cells treated with post 6-OHDA (100 μM) for 6 h. DPI significantly reduced 6-OHDA-mediated ROS generation. Representative photomicrograph of the blue formazan staining **(A)** and spectrophotometric quantitation of formazan showing ROS levels in various DPI concentrations under 6-OHDA treatment **(B). (C** and **D)** Apocynin reduced ROS generation as determined the NBT assay at 6 h post 6-OHDA (100 μM). Representative photomicrograph of the blue formazan staining **(C)** and spectrophotometric quantitation of formazan showing ROS levels in various apocynin concentrations under 6-OHDA treatment **(D)**. Results are presented as the mean + SEM; $n = 6$. The whole experiment has been repeated four times with similar results. $^{*}p < 0.05$; $^{**}p < 0.01$; $^{***}p < 0.001$. **(E** and **F)** RNAi-mediated Nox1 knockdown also significantly reduced 6-OHDA-induced ROS generation. **(E)** RNAi-mediated Nox1 knockdown efficiency was verified using both immunoblot analysis (*upper two panels*) and RT-PCR (*lower two panels*) in N27 cells transiently transfected with rat Nox1 siRNA or control siRNA for 36 h, followed by 6-OHDA exposure for 6 h. β-Actin and GAPDH were visualized as internal controls for immunoblot and RT-PCR, respectively. **(F)** ROS level was measured using the NBT assay; spectrophotometric quantitation of formazan between groups. Results are presented as the mean + SEM. $n = 6$. The whole experiment has been repeated four times with similar results. $^{***}p < 0.001$.

(Figs. 5C–5E). Increased 8-oxo-dG immunoreactivity in the presence of 6-OHDA was significantly reduced by pre-incubation of N27 cells with either Nox1 shRNA or T17NRac1/AAV2 viral particles. However, scramble shRNA failed to reduce 8-oxo-dG staining in the nucleus (Fig. 5C). As early as 3 days after striatal injection of 6-OHDA, 8-oxo-dG staining was increased in the SN (Fig. 5E). *In vivo* targeting of Rac1 or Nox1 was achieved by stereotaxic delivery of AAV2 particles harboring either T17NRac1 or Nox1shRNA into the rat SN. 6-OHDA was injected at 4 weeks post AAV2 injection which pointed out that, around 70% of TH + SNDA neurons were transduced with AAV2 particles as indicated by GFP. Immunostaining with 8-oxo-dG in the SN was reduced by either Nox1 knockdown or Rac1 inhibition (Fig. 5E), suggesting that Nox1/Rac1-derived superoxide generation is responsible for 6-OHDA-induced oxidative DNA damage. The fact that increased Nox1 expression is observed in the nucleus as early as 3 days post 6-OHDA (Fig. 4A) and increased nuclear 8-oxo-dG immunostaining (Fig. 5D) occurs concurrently, suggests that oxidative DNA damage is caused by Nox1/Rac1 activation. The results also suggest that Nox1-generated superoxide may play a critical role in oxidative damage to genomic DNA, which is frequently observed during both aging and in PD (32).

Inhibition of Rac1 or Nox1 reduced DA cell death induced by 6-OHDA

The next series of studies investigated the mechanism by which Nox1/Rac1- mediated DNA damage results in oxidative stress-induced DA neuronal death. c-Jun N-terminal kinase (JNK)-mediated signaling has been implicated as a final common pathway of DA neuronal apoptosis (42). Immunostaining of nuclear phospho c-jun (p-c-jun) was used as markers of 6-OHDA-induced apoptosis of DA cells. GFP-positive N27 cells expressing Nox1 shRNA lacked p-c-jun immunostaining (Figs. 6A and 6B), suggesting that Nox1

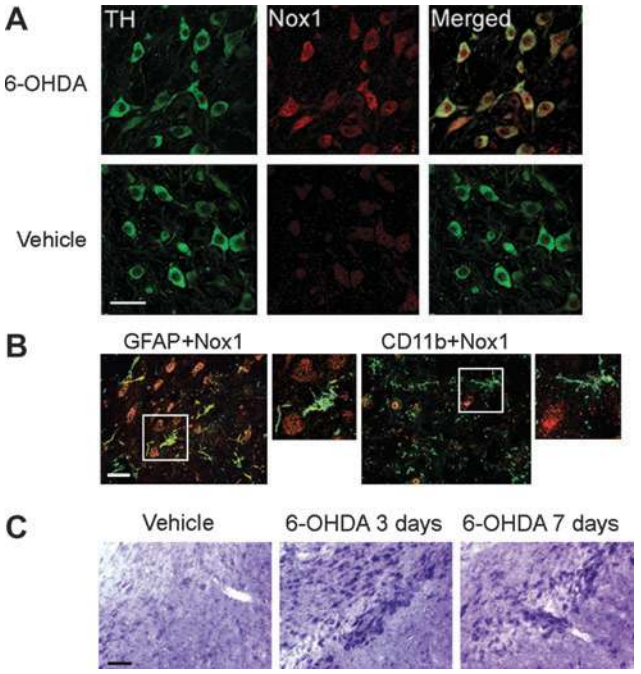

FIG. 3. Striatal administration of 6-OHDA robustly increased Nox1 expression in dopaminergic neurons in the SN. (A) Nox1 expression was increased in the rat SNDA neurons after 6-OHDA administration. TH (*green*) and Nox1 (*red*) were visualized in the rat SN at 3 days post-striatal injection of 6-OHDA (*upper panels*) or vehicle (*lower panels*). Nox1 expression in TH+ DA neurons is demonstrated as *yellow staining* after merging *green* (TH) and *red* (Nox1) images. Scale bars = 50 μm. **(B)** Nox1 (*red*) expression was observed neither in astrocytes nor in microglia. GFAP (*green*) and CD11b (*green*) were stained as markers for astrocytes and microglia, respectively. *Boxed area* is enlarged in the *right panel* of each staining. Scale bars = 30 μm. **(C)** Increased Nox1 mRNA level in the SN was detected by nonradioactive *in situ* hybridization at 3 days and 7 days post 6-OHDA administration. Scale bar = 150 μm.

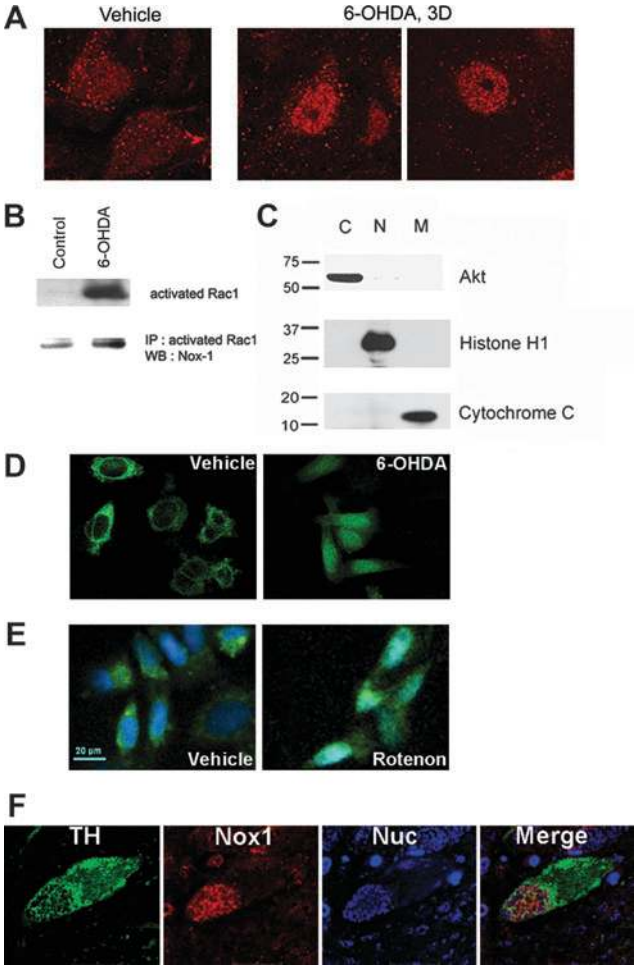

FIG. 4. Nuclear localization of Nox1. (A) Nox1 was visualized in the SN of rats 3 days after treatment with vehicle or 6-OHDA. **(B)** The nuclear fraction was prepared from N27 cells treated with 6-OHDA (50 μM) overnight. First, GTP bound Rac1 was determined using an active Rac1 pull-down assay (*upper panel*). Next, Nox1 was detected in the same blot (*lower blot*). **(C)** The purity of subcellular fractions was assessed using specific antibodies against Akt, histone H1, and cytochrome C for the cytoplasm (C), nucleus (N), and mitochondria (M), respectively. **(D)** N27 cells expressing Nox1-EGFP were treated with 6-OHDA (50 μM) for 6 h, and then subcellular localization of Nox1 was investigated by confocal microscopy. **(E)** N27 cells expressing Nox1-EGFP were treated with rotenone (5 μM) for 18 h, and then Nox1 nuclear localization was investigated. Nucleus was visualized with DAPI. **(F)** The SN area of human postmortem PD brain tissue was stained with TH (*green*), Nox1 (*red*), and TOTO (*blue*, nuclear). Nuclear localization of Nox1 was analyzed by confocal microscopy.

knockdown blocked 6-OHDA-mediated apoptosis in N27 cells. *In vivo*, a 4-week pre-injection with either Nox1 shRNA or T17NRac1/AAV2 viral particles in the SN area, significantly diminished SN DA neuronal loss produced by intrastriatal administration of 6-OHDA ($p < 0.01$) as determined by stereologic cell counting of tyrosine hydroxylase (TH)-immunostained DA neurons (Fig. 6C). Nox1 knockdown efficiency in the SN was verified by Western blot analysis (Supplementary Fig. 6). The number of Nissl-stained SNDA neurons also showed a similar protective effect. Direct injection of 6-OHDA into the rat SN resulted in a 90%–95% loss of TH-positive SNDA neurons in 2 weeks. Either Nox1 knockdown or Rac1 inhibition also significantly reduced DA neuronal death elicited by 6-OHDA ($p < 0.01$) (Supplementary Fig. 7). In similar experiments, the number of p-c-jun positive neurons in the SN of T17N Rac1- or Nox1 shRNA-expressing animals were significantly less than those in nontransduced animals, indicating that inhibition of Nox1/Rac1 activation attenuated 6-OHDA-elicited DA neuronal apoptosis in the SN (Fig. 6D). DA neuron-specific staining of p-c-jun was confirmed by co-immunostaining with TH (Supplementary Fig. 8).

Discussion

We present convincing evidence to support our hypothesis that the ROS produced by the Nox1/Rac1 complex play a pivotal role in the degeneration of nigrostriatal dopaminergic neurons in an animal model of PD. The accumulation of the Nox1 complex, production of ROS, and nuclear DNA damage are all found in the nucleus of degenerating dopaminergic neurons. In addition to these results, nuclear 8-oxo-dG staining precedes other signs of neuronal degeneration. These results strongly indicated that Nox1-mediated oxidative

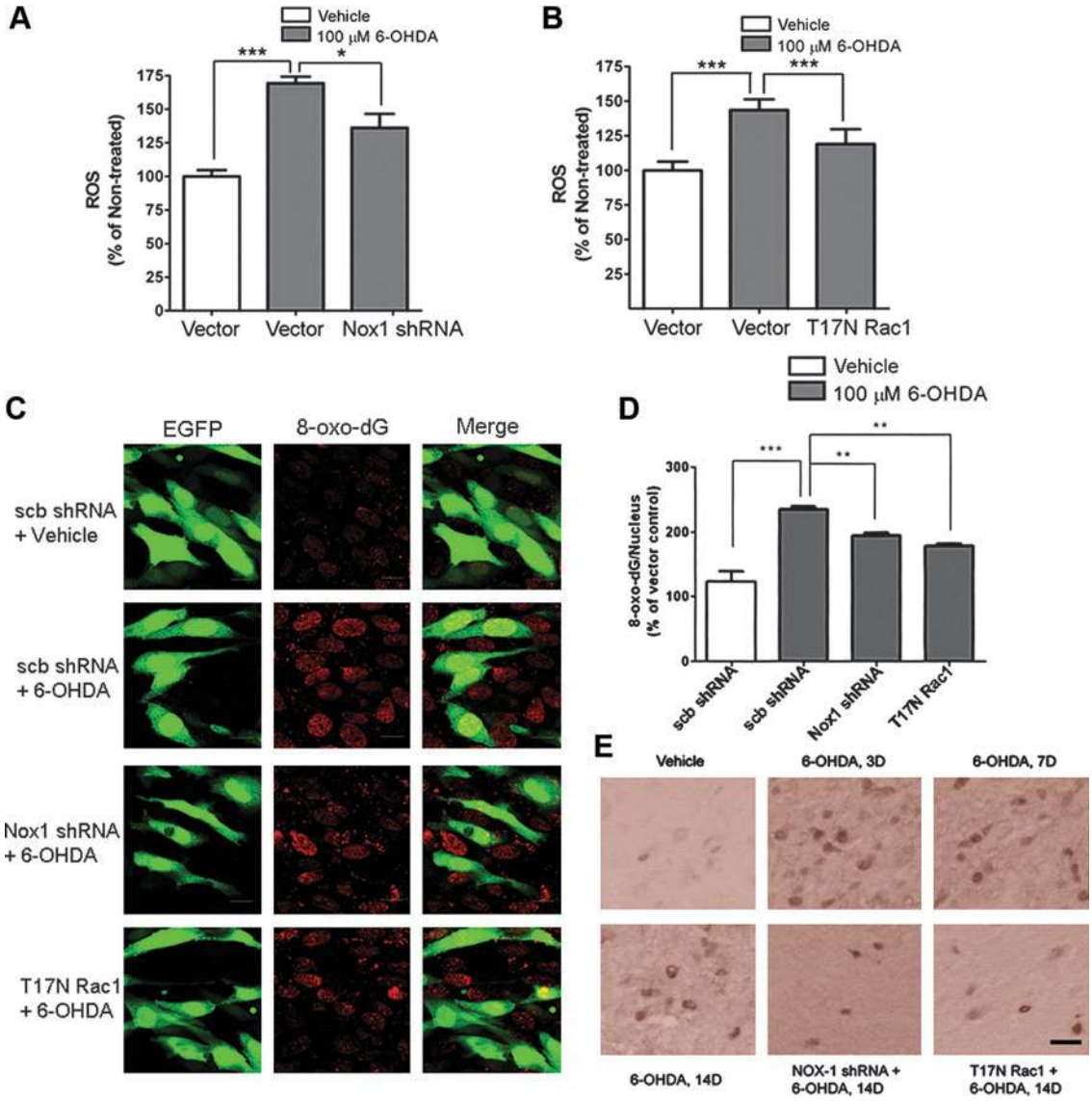

FIG. 5. Nox1 knockdown or Rac1 inhibition decreased 6-OHDA-induced ROS generation and DNA oxidative damage in dopaminergic cells. (A and **B)** N27 cells were incubated with Nox1 shRNA **(A)** or T17N Rac1/AAV particles **(B)** for 36 h and then exposed to 6-OHDA (100 μM) for 6 h. ROS levels were determined by the NBT assay and blue formazan was quantified. Results are presented as the mean + SEM; $n = 6$. The whole experiment was repeated 4 times with similar results. $^{*}p < 0.05$, $^{***}p < 0.001$. **(C)** N27 cells were incubated with either scramble shRNA/AAV, Nox1 shRNA/AAV, or T17N Rac1/AAV particles for 36 h and then exposed to 6-OHDA (100 μM) for 6 h. Oxidative DNA damage was detected by 8-oxo-dG immunostaining (*red*). Cells expressing GFP (*green*) represent AAV-transduced cells. scb shRNA, scramble shRNA/AAV. Representative images of four repeated experiments with similar results. **(D)** Under the same culture conditions described above, nuclear 8-oxo-dG-positive cells were counted. $^{**}p < 0.01$, $^{***}p < 0.001$. **(E)** 4 weeks after Nox1 shRNA or T17N Rac1/AAV injection into the rat SN, 6-OHDA was administered into the striatum. 14 days after 6-OHDA injection, 8-oxo-dG was detected in the SN (Nox1 shRNA + 6-OHDA 14D or T17N Rac1 + 6-OHDA 14D). Vehicle, vehicle for 14 days; 6-OHDA 3D, 7D, 14D, 3 days, 7 days, or 14 days after 6-OHDA administration, respectively. Scale bar = 30 μm.

damages may serve as critical upstream processes in neurodegeneration. Oxidative damage to DNA is the central issue in neurodegeneration. It is widely accepted that mitochondrial ROS causes oxidative damage to nuclear DNA; nonetheless, the mechanism underlying nuclear DNA damage is still elusive. We present in this current study critical evidence that ROS produced by the Nox1/Rac1 complex that accumulates in the nucleus, damages nuclear DNA which could be responsible for dopaminergic neurodegeneration. The evidences are: a) accumulation of the Nox1/Rac1 complex in the nucleus of both SN dopaminergic neurons in the 6-OHDA-treated rat model and dopaminergic cell cultures in presence of 6-OHDA; b) Nox1 expression in TH-positive neurons in the SN of the postmortem brain of PD patients; c) increased 8-oxo-dG staining in the nucleus, and subsequent attenuation of dopaminergic neurodegeneration either by chemical inhibition of Nox1 through apocynin, or by and genetic interventions targeting Nox1 and Rac1. Thus, our results lead to the new concept that oxidative damage to nuclear DNA occurs through the accumulation of Nox1/Rac1 complex and ROS in

the nucleus. This event is deleterious to dopaminergic neurons and to a new direction in the pursuit of an effective therapy for PD.

To selectively target Nox1/Rac1 in SN dopaminergic neurons *in vivo*, we developed the adeno-associated virus serotype 2 (AAV2)-mediated overexpression or knockdown system. Increasing reports including our recent study (12, 47) have shown that the AAV2-mediated gene transfer provides an effective means of achieving long-term expression of target genes in nondividing cells such as neurons (8) and that AAV-mediated shRNA delivery to the CNS for targeted knockdowns of specific genes can also be achieved successfully (37). Four weeks after an AAV injection into the rat SN, more than 70% of TH-positive neurons were GFP positive, indicating that our AAV system efficiently works in SN DA neurons. AAV2-mediated delivery of Nox1 shRNA or T17N Rac1 constructs similarly led to reduced DNA oxidative damage and a reduction of about 25%–30% in DA neuronal death induced by 6-OHDA.

It is noteworthy to mention here an important role of mitochondria in neurodegeneration along with Nox1 expression. Array of evidences suggest cross talk between mitochondria and transcriptional activation of Nox1 (16, 25, 28). In serum-deprived 293 cells, the early accumulation of mitochondrial ROS contributes to the sequential events of Nox1 induction and then the later phase of ROS accumulation followed by cell death (28). Studies of mitochondrial gene knockout osteosarcoma cells (ρ^0) revealed that the inactivation of mitochondrial genes leads to downregulation of Nox1 and that the transfer of wild-type mitochondrial genes can restore Nox1 expression (16). Our results also confirmed that mitochondrial respiratory chain inhibitors including rotenone, pyridaben, antimycin A, and FCCP, elevated both mRNA and protein levels of Nox1 (Supplementary Fig. 2). 6-OHDA directly generates free radicals by auto-oxidation and also serves as a potent inhibitor for the mitochondrial respiratory chain complexes I and IV (21). A recent study indicates that microglial NOX2-derived ROS synergistically contributes to 6-OHDA-induced DA cell death (38). ROS generated by 6-OHDA or mitochondrial events may also synergistically act on Nox1 induction and Rac1 activation in dopaminergic neurons and then, in turn, increase the ROS level and DA cell death. Establishing cooperative relationship between mitochondrial activity and Nox1 expression can be an important molecular event occurring in the toxin-elicited degeneration of SN dopaminergic neurons in both animal models of PD and the brain of PD patients.

Chronic exposure to ROS and the effects of ROS are devastating to neurons since damaged cells cannot be replaced by intact ones. Oxidative base modifications including damage and repair of DNA in both nuclear and mitochondria play a key role in the selective neuronal loss associated with mammalian aging and neurodegeneration. There are cell-type specific DNA repair systems and also differential DNA repair systems between mitochondria and the nucleus (34). For instance, oxidative base lesions in DNA are mainly repaired by base excision repair (BER) and mitochondrial uracil-DNA glycosylase 1 (UNG1) and nuclear uracil-DNA glycosylase 2 (UNG2) which are differentially regulated (1). Further studies on DNA damage and repair in mitochondria and the nucleus are required to elucidate the mechanisms underlying DNA damage-elicited neuronal degeneration in PD.

Dopaminergic neurons in SN are specific targets of environmental toxins that include toxic herbicides, such as paraquat, and it is suggested that human exposure to environmental toxins leads to sporadic neurodegenerative diseases, especially to PD. Earlier we have demonstrated that Nox1 is accumulated in SN dopaminergic neurons in paraquat-treated mice (13). This result, together with our current finding of the occurrence of Nox1 in SN dopaminergic neurons of the postmortem brain of PD patients, further strengthens our extended hypothesis that accumulation of Nox1 in SN dopaminergic neurons is a critical cellular event in developing neurodegeneration in PD.

An increasing number of studies has been identifying the specific localization of the members of the NOX family and their role in the CNS (43), and the dysregulation of the NOX system and ROS overproduction contribute to neuronal death and other diseases, such as cardiovascular diseases (24). Most of the NOX studies in neurodegenerative disease have highlighted microglial NOX2-induced ROS production. These studies include the cases of AD (36), ALS (29), and PD (49). Recent evidence indicates that oxidative stress may be caused directly from NOX in the neuron itself. Glutamate toxicity in SH-SY5Y neuroblastoma cells was largely attenuated by the inhibition of NOX activation (33). ROS generation and apoptosis of N27 DA cells treated with 1-methyl-4-phenylpyridinium (MPP+), active metabolite of MPTP, was also decreased by NOX inhibition (3). Nox1 is an inducible member of the NOX enzyme family and the Nox1 expression in cells may reflect the requirement of ROS for cellular homeostasis in quiescent states. Transcriptional activation of Nox1 in response to a variety of stimuli has been described in various tissues (18, 19, 26). We also observed that Nox1 expression was significantly increased after exposure to various toxic insults in N27 rat dopaminergic cells. Both Nox1 mRNA and protein increase under oxidative stressed conditions such as 6-OHDA, rotenone, and H_2O_2. Nox1 is constitutively expressed at a low level *in vivo* in SN dopaminergic neurons. In a parallel culture of N27 cells, both mRNA transcript and protein levels of Nox1 are increased mostly in (or exclusively) SN dopaminergic neurons of 6-OHDA-treated rats. Although Nox4 was constitutively expressed in N27 cells, we failed to detect Nox4 transcript in the rat SN dopaminergic neurons *in vivo*.

The most interesting finding here is the nuclear localization of Nox1/Rac1 complex and the subsequent oxidative damage to DNA. Distinct subcellular localizations of Nox1 in non-neuronal cells have been reported (10, 16, 23). The aforementioned study using osteosarcoma cells showed the presence of Nox1 in mitochondria (16). While Nox1 is found in the cellular periphery in human vascular smooth muscle cells, it is localized to the nucleus in transformed human keratinocytes (10, 23). Recent study demonstrated that Nox4 is localized to the nucleus and responsible for DNA oxidative damage, as well as MCP-1 expression in hemangioendotheliomas (22). In N27 cells treated with 6-OHDA, the GTP-bound Rac1 and its binding to Nox1 in the nucleus were increased. In the rat SN dopaminergic neurons, Nox1 expression is increased in the nucleus as early as 3 days post 6-OHDA treatments. At this time point, TH-positive dopaminergic neuronal loss was not observed, but nuclear 8-oxo-dG is densely stained, suggesting that oxidative nuclear DNA damage precedes neuronal degeneration. The low-level nuclear expression of Nox1 under unstressed conditions may contribute to redox-responsive gene expression necessary for cellular homeostasis (5). Nox1 does not contain a putative nuclear localization sequence

(NLS), suggesting that its nuclear translocation may be dependent on other molecules which form an enzyme complex with Nox1. Rac1 has a NLS in the C-terminus and thus translocates to the nucleus upon activation (30). Noxo1 gamma was also found in the nucleus (46). It needs to be clarified whether Rac1 activation is independently responsible for Nox1/Rac1 translocation into the nucleus or its co-localization in the nucleus. The major pathway responsible for removing oxidative DNA damage and restoring the integrity of the genome is base excision repair (BER), and defective BER

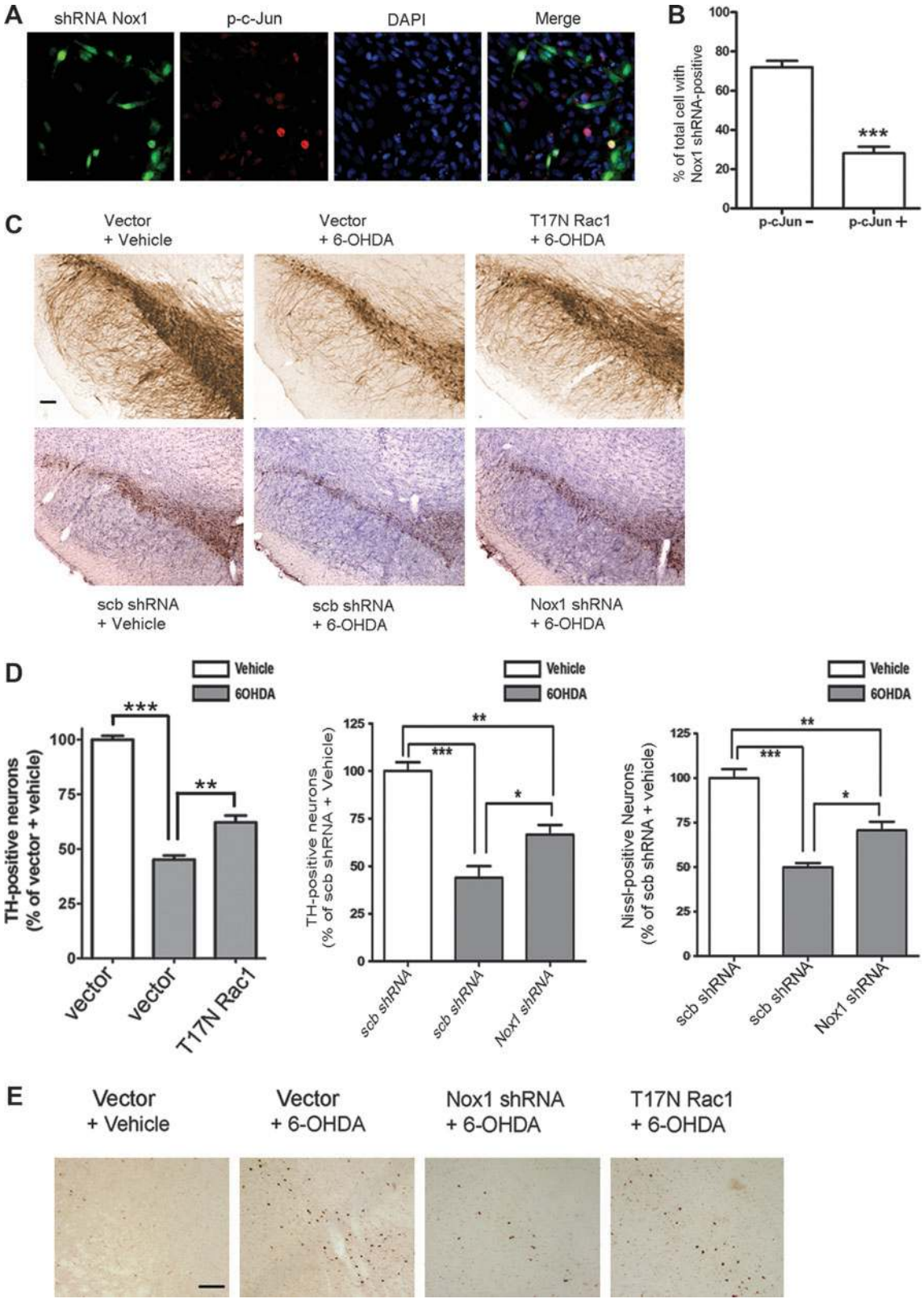

processing can promote neuronal cell death and neurodegenerative disease (1). This line of study is required for further understanding of the molecular mechanisms underlying neuronal degeneration through nuclear DNA damage in PD. The mechanism underlying nuclear translocation of Nox1 and active Rac1 in DA neurons also requires further investigation.

Materials and Methods

N27 cell culture

N27 cells are derived from rat mesencephalon and express tyrosine hydroxylase and dopamine transporter (35). Cells were grown in RPMI 1640 containing 10% FBS, 100 IU/l penicillin, and 10 g/ml streptomycin at 37°C with 5% CO_2 supply in humidified atmosphere. For experiments, the cells were plated on polystyrene tissue culture dishes at a density of 2×10^4 cells/well in 96-well culture plates, 1×10^5 cells/well in 24-well culture plates, 1×10^6 cells/well in 6-well culture plates, or 2×10^6 cells/100 mm plate. After 24 h, the cells were fed with fresh medium and treated with 6-OHDA and/or other drugs.

Total RNA extraction and RT-PCR analysis

Total RNA was extracted from N27 cells using Trizol reagent (Invitrogen, Carlsbad, CA). Reverse transcription was performed for 1 h at 42°C with 1 μg of total RNA using 20 unit/μl of AMV reverse transcriptase (Roche Applied Science, Indianapolis, IN), and oligo-p$(dT)_{15}$ as a primer. The samples were then heated at 99°C for 5 min to terminate the reaction. The cDNA obtained from 1 μg total RNA was used as a template for PCR amplification. Oligonucleotide primers were designed based on Genebank entries for rat NOX1 (sense, 5′-TGAC AGTGATGTATGCAGCAT-3′; antisense, 5′-CAGCTTGTTGT GTGCACGCTG-3′), rat NOX2 (sense, 5′-ACTCGAAAACTT CTTGGGTCAG-3′; antisense, 5′-TCCTGTGATGCCAGCCAA CCGAG-3′), rat NOX4 (sense, 5′-GCCGGCGGTATGGCGCT GTC-3′; antisense, 5′-CCACCATGCAGACACCTGTCAGG-3′), rat NOXA1 (sense, 5′-TCTAGGGGATCAGATACGGGAC-3′; antisense, 5′-CCAAGGAAATCCATGGGCTCCAG-3′), rat NOXO1 (sense, 5′-ACCCAGTATCAGCCCATGCTG-3′; antisense, 5′- ATGGAGCATCAGGAAGCTTGG-3′), rat p47 (sense, 5′-GTTAAAGGAGATGTTCCCCATTG-3′; antisense, 5′-TTAT GAATGACCTCGATGGCTTC-3′), rat Duox1 (sense, 5′-AGTA GGGGATTGGGG AT-3′; antisense, 5′-TCTATAAGTGGCCC CTGGCT-3′), rat Duox2 (sense, 5′-GACCTGGATGGAAATG GCTT-3′; antisense, 5′-ACTCGACAGGCATTGCTTTG-3′) and rat GAPDH (sense, 5′-ATCACCATCTTCCAGGAGCG-3′; antisense, 5′-GATGGCATGGACTGTGGTCA-3′). PCR mixes contained 10 μl of 2X PCR buffer, 1.25 m*M* of each dNTP, 10 pmol of each forward and reverse primer, and 2.5 units of Taq polymerase in the final volume of 20 μl. Amplification was performed in 35 cycles at 60°C, 30 sec; 72°C, 1 min; 94°C, 30 sec. After the last cycle, all samples were incubated for an additional 10 min at 72°C for final extension step. PCR fragments were analyzed on 1.2% agarose gel in 0.5×TAE containing ethidium bromide. Amplification of GAPDH, a relatively invariant internal reference RNA, was performed in parallel, and cDNA amounts were normalized against GAPDH mRNA levels. The primer set specifically recognized only the gene of interest as indicated by amplification of a single band of expected size.

Western blot analysis

Cells were washed with ice-cold PBS and lysed on ice in RIPA buffer (1% PBS, 1% NP-40, 0.5% sodium deoxycholate, 0.1% SDS) containing protease inhibitor mixture (AEBSF, aprotinin, bestatin hydrochloride, E-64-[N-(trans-epoxysuccinyl)-L-leucine 4-guanidinobutylamide], leupeptin, pepstatin A) (Sigma, Saint Louis, MO). A total of 30 μg of soluble protein per lane was loaded in SDS-PAGE and electrotransferred onto PVDF membrane. Specific protein bands were detected by using specific anti-Nox1 antibody (Santa Cruz Biotechnology, Santa Cruz, CA) and Enhanced Chemiluminescence (Pierce, Rockford, IL).

Determination of ROS using NBT staining

6-OHDA treated cells were incubated for 1 h at 37°C with a filtered solution of 0.3 mg/ml of NBT in complete medium. The cells were washed once with PBS and fixed with 0.4% paraformaldehyde for light microscopy. To quantify NBT precipitation, cells were washed twice with 70% methanol and fixed for 5 min in 100% methanol. After the wells were allowed to dry in the air, the formazan is solubilized with 120 μl 2 *M* K OH and 140 μl DMSO. The OD was read in an ELISA plate reader at 590 nm.

Rac1 activation assay

Total cellular protein (500 μg) obtained from lysed N27 cells was incubated with 20 μl of agarose beads containing p21-binding domain (PBD) of p21-activated protein kinase 1 (PAK1), an effector of activated Rac, for 1 h at 48°C. The beads

FIG. 6. Decreased DA cell death by Nox1 knockdown or Rac1 inhibition. (A and **B)** N27 cells were incubated with Nox1 shRNA/ AAV particles for 36 h and then exposed to 6-OHDA (100 μM) for 6 h. Cultures were stained with phospho-c-Jun (p-c-Jun, *red*). Cells expressing GFP (*green*) represent AAV-transduced cells. DAPI staining (*blue*) was used to visualize nucleus **(A)**. GFP-positive and p-c-Jun-negative cells (p-c-Jun-, *green*) and GFP-positive and p-c-Jun-positive cells (p-c-Jun+, *yellow*) cells were counted. Total 726 GFP-positive cells were counted. Data represent three independent experiments with similar results. ***$p<0.001$ **(B). (C** and **D)** Representative photomicrographs of TH staining in the rat SN sections. AAV particles containing empty vector, scramble shRNA, Nox1 shRNA, or T17NRac1 were stereotaxically injected into the rat SN. After 4 weeks incubation, vehicle or 6-OHDA were injected into the striatum. Two weeks later, DA neurons in the SN were visualized with TH immunostaining (*upper panel*) for T17N Rac1. For Nox1 shRNA, the SN was stained both TH and Nissl. Vector, injection of vector/AAV particles into the SN; T17N Rac1, injection of T17NRac1/AAV particles into the SN; scb shRNA, injection of scramble shRNA/AAV into the SN; Nox1 shRNA, injection of Nox1 shRNA/AAV particles into the SN; + vehicle, striatal injection of vehicle 4 weeks after AAV; + 6-OHDA, striatal injection of 6-OHDA 4 weeks after AAV. Scale bar = 150 μm **(C)**. Stereologic counts of TH-positive neurons in the SN shown as percentage of vector + vehicle or scb shRNA + vehicle (*left and middle panel*). Nissle-positive neurons in the SN shown as percentage of scb shRNA + vehicle. Results are presented as the mean + SEM. $n = 6–7$. Significance is indicated by ***$p<0.001$ and **$p<0.01$ **(D). (E)** p-c-Jun was also detected in the SN by immunohistochemistry. Scale bar = 100 μm.

were collected by centrifugation and washed two times in the lysis buffer, resuspended in sample buffer. and boiled for 5 min. Proteins were resolved by SDS-PAGE using a 10%–20% Tricine gel, transferred electrophoretically and visualized using anti-rat Rac1 antibody, followed by electrochemoluminescence (ECL) detection. For the positive control, the nonhydrolyzable GTP analog GTPgS was used according to the manufacturer's protocol (Cell Biolabs, New York, NY).

Preparation and transfection of siRNA

Sense and anti-sense oligonucleotides corresponding to the following cDNA sequences of rat Nox1 were used (5'-CCTTTGCTTCCTTCTTGAAATCTAT-3'). The double-stranded siRNAs were synthesized chemically and modified into stealth siRNA (Invitrogen, Carlsbad, CA) to enhance the stability *in vitro*. Negative control stealth RNAi with a similar GC content as Nox1 stealth RNAi was used. The sense and anti-sense oligonucleotides were annealed following the manufacturer's protocol to generate double-stranded siRNAs at the final concentration of 20 μM. N27 cells grown to 80% confluence in 6-well culture plates were subjected to transfection by adding 10 μl of Lipofectamin TM 2000 and 8 μl of 20 μM siRNAs (final concentration 40 nM). After 6 h of incubation, the culture medium was changed and cells were maintained for additional 30 h before analysis.

Lactate dehydrogenase assay

Degrees of cell death were assessed by activity of LDH released into the culture medium using the cytotoxic assay kit (Promega Bioscience, San Luis Obispo, CA). Aliquots (50 μl) of cell culture medium were incubated with 50 μl of LDH substrates for 15 ~ 30 min at room temperature. The rate of NAD^+ formation was monitored for 5 min at 2-sec intervals at 340 nm using a microplate spectrophotometer (Spectra Max 340 pc; Molecular Devices, Menlo Park, CA).

Animals and stereotaxic injection of AAV2 particles and 6-OHDA

The experiments were carried out on rats, in accordance with the NIH Guide for the Care and Use of Laboratory Animals. All procedures were approved by the local Animal Care and Use Committee. Female Sprague Dawley (SD) rats (Charles River; 8-weeks-old at the time of the beginning of AAV expression or 6-OHDA treatment, 2 or 3 per cage) were maintained in a temperature/humidity-controlled environment under a 12 h light/dark cycle with free access to food and water. All rats were respectively allocated into 2 groups, Nox1 shRNA/AAV, T17N Rac1/AAV, and scramble (scb) shRNA/AAV or empty vector/AAV as control groups. Rats were deeply anesthetized (ketamine and xylazine mixture 30 mg/kg, *i.p.*) and placed in a rat stereotaxic apparatus, a site in the right substantia nigra (SN) [coordinate: anteroposterior (AP), –5.3 mm; mediolateral (ML), +2.0 mm; dorsoventral (DV), –5.8 mm] was selected to inject scb shRNA/AAV ($n=8$), Nox1 shRNA/AAV ($n=16$), T17N Rac1/AAV ($n=16$), and empty vector/AAV ($n=28$), respectively, according to the grouping. A total of 1×10^{11} genome copy/ml rAAV particles encoding shNox1, T17N rac1, scb, or empty vector diluted in 2 μl ice-cold sterilized phosphate buffered saline (PBS) were used in every animal. Four animals of Nox1 shRNA/AAV, T17N Rac1/AAV, or empty vector group were used for the detection of Nox1 shRNA, T17N Rac1, or empty vector expression at 4 weeks following AAV particle injection. Six animals received ipsilateral injection of 0.02% ascorbic acid while all other rats received ipsilateral injection of freshly prepared 2 μl of 6-hydroxydopamine (6-OHDA, Sigma) at the concentration of 7.5 μg/μl containing 0.02% ascorbic acid at two coordinates in the right striatum (coordinate: AP, +0.7 mm; ML, +2.2 mm and +2.0 mm; DV, –5.0 mm). The injection rate was 0.5 μl/min, and the syringe was kept in place for an additional 5 min before being retracted slowly. Rats were sacrificed after 3, 5, and 14 days (6 rats per time point).

Immunohistochemistry

Rats were deeply anesthetized with sodium pentobarbital (120 mg/kg) and transcardially perfused with saline containing 0.5% sodium nitrite and 10 U/ml heparin sulfate, followed by 4% cold formaldehyde generated from paraformaldehyde in 0.1 *M* PBS (pH 7.2). Brains were post-fixed in the same solution for overnight and infiltrated with 30% sucrose overnight. Free-floating sections (40 μm) were obtained from the striata and SN using a Cryostat. Sections were washed in 0.1 *M* PBS, incubated in 0.1 *M* PBS containing 5% normal goat serum and 0.3% TritonX-100 for 1 h, and subsequently incubated overnight with TH (1:10,000), MDA (1:1000), or p-c-jun (1:1,000) antibodies at 4°C. For 7,8-dihydro-8-oxo-deoxyguanine (8-oxo-dG) staining, brain slides were incubated in 70% ethanol precooled to −20°C for 10 min on ice followed by 4 *N* HCl to denature DNA. After rinsing with PBS, the slides were soaked in 37°C PBS supplemented with 100 μg/ml DNase-free RNase A for 1 h. Blocking for immunostaining was done in PBS containing 5% FBS, 5% horse serum, and 0.05% Triton-X100 for 2 h. The slides were incubated with primary mouse anti-8-oxo-dG antibody (1:300) in PBS containing 2.5% FBS, 2.5% horse serum, and 0.05% Triton-X-100 overnight at 4°C. The sections were then incubated with appropriate secondary IgG (1:200) for 1 h, followed by avidin/biotin/peroxidase staining for 1 h in a humidified chamber. Washing of the sections on slides was done using 0.1 *M* PBS containing 1.5% bovine serum albumin that was used to wash sections between all steps. The antigen–antibody complexes were visualized by incubation for 5 min in 0.05% 3,3'-diaminobenzidine and 0.003% H_2O_2. Nissl staining was performed by incubation of sections in 0.1% Cresyl violet solution for 5–10 min at room temperature and rinsed quickly in distilled water, and dehydrated in serially diluted ethanol, and cleaned in xylene followed by sequential mounting in glass slides using permanent mounting medium. Mounted slices were evaluated on light microscope.

Double-fluorescent immunostaining of tissues

Free-floating sections (40 μm) were washed in 0.1 *M* PBS, incubated in 0.1 *M* PBS containing 5% normal donkey serum and 0.3 % TritonX-100 for 1 h, and subsequently incubated overnight with primary antibodies (TH, 1:2,000; Nox1, 1:200; GFAP, 1:500; CD11b, 1:200) in 2% normal donkey serum in PBS at 4°C and incubated in a 1:200 dilution of AlexaFluor conjugated donkey anti-rabbit (546) or donkey anti-mouse (488) antibodies for 1h at room temperature, washed with PBS, incubated in TOTO-3 (1:1,000) in 0.1 *M* PBS for 5 min,

and then mounted sequentially in glass slides using Vectashield. Mounted slices were evaluated for fluorescence under settings for 546, 488, and 660 nm emissions on a confocal microscope (Leica TCS SP5).

TH immunostaining and TH- positive cells counting

A set consisting of six sections, 360 μm apart, were prepared. Sections were used for tyrosine hydroxylase (TH) immunohistochemistry using avidin–biotin peroxidase technique (Vectastain ABC kit from Vector Labs, Burlingame, CA). A rabbit anti-TH affinity purified antibody (1: 10,000; from Protos Biotech, New York, NY) was used. Numbers of TH-immunoreactive cells in the substantia nigra (SN) were counted using the optical fractionator (47a). Analysis was performed using a system consisting of a Nikon Eclipse E600 microscope (Morrell Instruments Co. Inc., Melville, NY) equipped with a computer-controlled LEP BioPoint motorized stage (Ludl Electronic Products, Hawthorne, NY), a DEI-750 video camera (Meyer Instruments, Houston, TX), a Dell Dimension 4300 computer (Dell, Round Rock, TX), and the Stereo Investigator (v. 4.35) software program (Microbrightfield, Burlington, VT). Tissue sections were examined using a Nikon Plan Apo 100·objective lens with a 1.4 numerical aperture. The size of the x–y sampling grid was 140μm. The counting frame thickness was 30 μm and the counting frame area was 4900 μm^2. The coefficient of error and coefficient of variation were also determined.

Immunocytochemistry

For fluorescent immunostaining, N27 cells in the 4-well chamber slide were incubated for 1 h at 37°C in 2% normal donkey serum containing either a rabbit polyclonal antibody against Nox1 (1:500), or p-c-jun (1:500). For 7,8-dihydro-8-oxo-deoxyguanine (8-oxo-dG) staining, slides were incubated in 70% ethanol pre-cooled to −20°C for 10 min on ice. After rinsing with PBS, the slides were soaked in 37°C PBS supplemented with 100 mg/ml RNase A, DNase-free for 1 h. Blocking for immunostaining was done in PBS containing 5% FBS, 5% horse serum, and 0.05 % Triton-X100 for 2 h. The slides were incubated with primary mouse anti-8-oxo-dG antibody (1:300) in PBS containing 2.5% FBS, 2.5% horse serum, and 0.05% Triton- X-100 overnight at 4°C. Specific binding was detected by incubation for 60 min at room temperature with a 1:200 dilution of secondary antibodies conjugated to AlexaFluor 546 dyes. For determination of cell death, cells were stained with the TdT-mediated dUTP-X nick end labeling (TUNEL) reaction mixture (Roche Applied Science) that contains TdT and TMR (fluorescein-labeled) –dUTP for 60 min at 37°C in a humidified atmosphere in the dark. Slides were washed with 0.1 *M* PBS and then mounted sequentially in glass slides using Vectashield (Vector Labs). Mounted slices were evaluated for fluorescence under settings for 546 and 488 nm emissions on a confocal microscope.

Data analysis

Data were expressed as means + standard error of the mean (SEM) and were analyzed using one way analysis of variance (ANOVA) and Student–Newman–Keul's test for individual comparisons. *P* values less than 0.05 were considered statistically significant.

Acknowledgments

We thank Drs. Kwang-Soo Kim and Seok-Jong Hong for advice with the AAV system and Dr. Harriet Baker for her careful review of the manuscript. This work is partly supported by the US National Institute of Health (RO1 NS062827-01A2 grant to YSK), Michael J. Fox Foundation (Target Validation 2009 grant to YSK) and Basic Science Research Program through the National Research Foundation of Korea (NRF) funded by the Ministry of Education, Science and Technology (2009-0070536 grant to DHC).

Author Disclosure Statement

The authors declare that they have no competing financial interests.

References

1. Akbari M, Otterlei M, Pena-Diaz J, and Krokan HE. Different organization of base excision repair of uracil in DNA in nuclei and mitochondria and selective upregulation of mitochondrial uracil-DNA glycosylase after oxidative stress. *Neuroscience* 145: 1201–1212, 2007.
2. Alam ZI, Jenner A, Daniel SE, Lees AJ, Cairns N, Marsden CD, Jenner P, and Halliwell B. Oxidative DNA damage in the parkinsonian brain: An apparent selective increase in 8-hydroxyguanine levels in substantia nigra. *J Neurochem* 69: 1196–1203, 1997.
3. Anantharam V, Kaul S, Song C, Kanthasamy A, and Kanthasamy AG. Pharmacological inhibition of neuronal NADPH oxidase protects against 1-methyl-4-phenylpyridinium (MPP+)-induced oxidative stress and apoptosis in mesencephalic dopaminergic neuronal cells. *Neurotoxicology* 28: 988–997, 2007.
4. Banfi B, Clark RA, Steger K, and Krause KH. Two novel proteins activate superoxide generation by the NADPH oxidase NOX1. *J Biol Chem* 278: 3510–3513, 2003.
5. Bedard K and Krause KH. The NOX family of ROS-generating NADPH oxidases: Physiology and pathophysiology. *Physiol Rev* 87: 245–313, 2007.
6. Behrens MM, Ali SS, Dao DN, Lucero J, Shekhtman G, Quick KL, and Dugan LL. Ketamine-induced loss of phenotype of fast-spiking interneurons is mediated by NADPH-oxidase. *Science* 318: 1645–1647, 2007.
7. Bender A, Krishnan KJ, Morris CM, Taylor GA, Reeve AK, Perry RH, Jaros E, Hersheson JS, Betts J, Klopstock T, Taylor RW, and Turnbull DM. High levels of mitochondrial DNA deletions in substantia nigra neurons in aging and Parkinson disease. *Nat Genet* 38: 515–517, 2006.
8. Bjorklund A, Kirik D, Rosenblad C, Georgievska B, Lundberg C, and Mandel RJ. Towards a neuroprotective gene therapy for Parkinson's disease: Use of adenovirus, AAV and lentivirus vectors for gene transfer of GDNF to the nigrostriatal system in the rat Parkinson model. *Brain Res* 886: 82–98, 2000.
9. Bokoch GM and Diebold BA. Current molecular models for NADPH oxidase regulation by Rac GTPase. *Blood* 100: 2692–2696, 2002.
10. Chamulitrat W, Schmidt R, Tomakidi P, Stremmel W, Chunglok W, Kawahara T, and Rokutan K. Association of gp91phox homolog Nox1 with anchorage-independent growth and MAP kinase-activation of transformed human keratinocytes. *Oncogene* 22: 6045–6053, 2003.

11. Cheng G, Cao Z, Xu X, van Meir EG, and Lambeth JD. Homologs of gp91phox: cloning and tissue expression of Nox3, Nox4, and Nox5. *Gene* 269: 131–140, 2001.
12. Choi DH, Kim YJ, Kim YG, Joh TH, Beal MF, and Kim YS. Role of matrix metalloproteinase 3-mediated alpha-synuclein cleavage in dopaminergic cell death. *J Biol Chem* 286: 14168–14177, 2011.
13. Cristovao AC, Choi DH, Baltazar G, Beal MF, and Kim YS. The role of NADPH oxidase 1-derived reactive oxygen species in paraquat-mediated dopaminergic cell death. *Antioxid Redox Signal* 11: 2105–2118, 2009.
14. Daiber A. Redox signaling (cross-talk) from and to mitochondria involves mitochondrial pores and reactive oxygen species. *Biochim Biophys Acta* 1797: 897–906, 2010.
15. De Deken X, Wang D, Many MC, Costagliola S, Libert F, Vassart G, Dumont JE, and Miot F. Cloning of two human thyroid cDNAs encoding new members of the NADPH oxidase family. *J Biol Chem* 275: 23227–23233, 2000.
16. Desouki MM, Kulawiec M, Bansal S, Das GM, and Singh KK. Cross talk between mitochondria and superoxide generating NADPH oxidase in breast and ovarian tumors. *Cancer Biol Ther* 4: 1367–1373, 2005.
17. Edens WA, Sharling L, Cheng G, Shapira R, Kinkade JM, Lee T, Edens HA, Tang X, Sullards C, Flaherty DB, Benian GM, and Lambeth JD. Tyrosine cross-linking of extracellular matrix is catalyzed by Duox, a multidomain oxidase/peroxidase with homology to the phagocyte oxidase subunit gp91phox. *J Cell Biol* 154: 879–891, 2001.
18. Fan CY, Katsuyama M, and Yabe-Nishimura C. PKCdelta mediates up-regulation of NOX1, a catalytic subunit of NADPH oxidase, via transactivation of the EGF receptor: Possible involvement of PKCdelta in vascular hypertrophy. *Biochem J* 390: 761–767, 2005.
19. Geiszt M, Lekstrom K, Brenner S, Hewitt SM, Dana R, Malech HL, and Leto TL. NAD(P)H oxidase 1, a product of differentiated colon epithelial cells, can partially replace glycoprotein 91phox in the regulated production of superoxide by phagocytes. *J Immunol* 171: 299–306, 2003.
20. Geiszt M, Lekstrom K, Witta J, and Leto TL. Proteins homologous to p47phox and p67phox support superoxide production by NAD(P)H oxidase 1 in colon epithelial cells. *J Biol Chem* 278: 20006–20012, 2003.
21. Glinka Y, Gassen M, and Youdim MB. Mechanism of 6-hydroxydopamine neurotoxicity. *J Neural Transm Suppl* 50: 55–66, 1997.
22. Gordillo G, Fang H, Park H, and Roy S. Nox-4-dependent nuclear H2O2 drives DNA oxidation resulting in 8-OHdG as urinary biomarker and hemangioendothelioma formation. *Antioxid Redox Signal* 12: 933–943.
23. Hilenski LL, Clempus RE, Quinn MT, Lambeth JD, and Griendling KK. Distinct subcellular localizations of Nox1 and Nox4 in vascular smooth muscle cells. *Arterioscler Thromb Vasc Biol* 24: 677–683, 2004.
24. Infanger DW, Sharma RV, and Davisson RL. NADPH oxidases of the brain: Distribution, regulation, and function. *Antioxid Redox Signal* 8: 1583–1596, 2006.
25. Katsuyama M, Fan C, Arakawa N, Nishinaka T, Miyagishi M, Taira K, and Yabe-Nishimura C. Essential role of ATF-1 in induction of NOX1, a catalytic subunit of NADPH oxidase: Involvement of mitochondrial respiratory chain. *Biochem J* 386: 255–261, 2005.
26. Kawahara T, Kohjima M, Kuwano Y, Mino H, Teshima-Kondo S, Takeya R, Tsunawaki S, Wada A, Sumimoto H, and Rokutan K. *Helicobacter pylori* lipopolysaccharide activates Rac1 and transcription of NADPH oxidase Nox1 and its organizer NOXO1 in guinea pig gastric mucosal cells. *Am J Physiol Cell Physiol* 288: C450–457, 2005.
27. Kuroda J, Nakagawa K, Yamasaki T, Nakamura K, Takeya R, Kuribayashi F, Imajoh-Ohmi S, Igarashi K, Shibata Y, Sueishi K, and Sumimoto H. The superoxide-producing NAD(P)H oxidase Nox4 in the nucleus of human vascular endothelial cells. *Genes Cells* 10: 1139–1151, 2005.
28. Lee SB, Bae IH, Bae YS, and Um HD. Link between mitochondria and NADPH oxidase 1 isozyme for the sustained production of reactive oxygen species and cell death. *J Biol Chem* 281: 36228–36235, 2006.
29. Marden JJ, Harraz MM, Williams AJ, Nelson K, Luo M, Paulson H, and Engelhardt JF. Redox modifier genes in amyotrophic lateral sclerosis in mice. *J Clin Invest* 117: 2913–2919, 2007.
30. Michaelson D, Abidi W, Guardavaccaro D, Zhou M, Ahearn I, Pagano M, and Philips MR. Rac1 accumulates in the nucleus during the G2 phase of the cell cycle and promotes cell division. *J Cell Biol* 181: 485–496, 2008.
31. Migliore L, Petrozzi L, Lucetti C, Gambaccini G, Bernardini S, Scarpato R, Trippi F, Barale R, Frenzilli G, Rodilla V, and Bonuccelli U. Oxidative damage and cytogenetic analysis in leukocytes of Parkinson's disease patients. *Neurology* 58: 1809–1815, 2002.
32. Nakabeppu Y, Tsuchimoto D, Yamaguchi H, and Sakumi K. Oxidative damage in nucleic acids and Parkinson's disease. *J Neurosci Res* 85: 919–934, 2007.
33. Nikolova S, Lee YS, and Kim JA. Rac1-NADPH oxidase-regulated generation of reactive oxygen species mediates glutamate-induced apoptosis in SH-SY5Y human neuroblastoma cells. *Free Radic Res* 39: 1295–1304, 2005.
34. Nouspikel T. DNA repair in differentiated cells: Some new answers to old questions. *Neuroscience* 145: 1213–1221, 2007.
35. Prasad KN, Carvalho E, Kentroti S, Edwards-Prasad J, Freed C, and Vernadakis A. Establishment and characterization of immortalized clonal cell lines from fetal rat mesencephalic tissue. *In Vitro Cell Dev Biol Anim* 30A: 596–603, 1994.
36. Qin B, Cartier L, Dubois-Dauphin M, Li B, Serrander L, and Krause KH. A key role for the microglial NADPH oxidase in APP-dependent killing of neurons. *Neurobiol Aging* 27: 1577–1587, 2006.
37. Rodriguez-Lebron E, Denovan-Wright EM, Nash K, Lewin AS, and Mandel RJ. Intrastriatal rAAV-mediated delivery of anti-huntingtin shRNAs induces partial reversal of disease progression in R6/1 Huntington's disease transgenic mice. *Mol Ther* 12: 618–633, 2005.
38. Rodriguez-Pallares J, Parga JA, Munoz A, Rey P, Guerra MJ, and Labandeira-Garcia JL. Mechanism of 6-hydroxydopamine neurotoxicity: The role of NADPH oxidase and microglial activation in 6-hydroxydopamine-induced degeneration of dopaminergic neurons. *J Neurochem* 103: 145–156, 2007.
39. Rossi F and Zatti M. Biochemical aspects of phagocytosis in polymorphonuclear leucocytes. NADH and NADPH oxidation by the granules of resting and phagocytizing cells. *Experientia* 20: 21–23, 1964.
40. Schapira AH, Cooper JM, Dexter D, Jenner P, Clark JB, and Marsden CD. Mitochondrial complex I deficiency in Parkinson's disease. *Lancet* 1: 1269, 1989.
41. Sherer TB and Greenamyre JT. Oxidative damage in Parkinson's disease. *Antioxid Redox Signal* 7: 627–629, 2005.
42. Silva RM, Kuan CY, Rakic P, and Burke RE. Mixed lineage kinase-c-jun N-terminal kinase signaling pathway: A new therapeutic target in Parkinson's disease. *Mov Disord* 20: 653–664, 2005.

43. Sorce S and Krause KH. NOX enzymes in the central nervous system: From signaling to disease. *Antioxid Redox Signal* 11: 2481–2504, 2009.
44. Stolk J, Hiltermann TJ, Dijkman JH, and Verhoeven AJ. Characteristics of the inhibition of NADPH oxidase activation in neutrophils by apocynin, a methoxy-substituted catechol. *Am J Respir Cell Mol Biol* 11: 95–102, 1994.
45. Suh YA, Arnold RS, Lassegue B, Shi J, Xu X, Sorescu D, Chung AB, Griendling KK, and Lambeth JD. Cell transformation by the superoxide-generating oxidase Mox1. *Nature* 401: 79–82, 1999.
46. Ueyama T, Lekstrom K, Tsujibe S, Saito N, and Leto TL. Subcellular localization and function of alternatively spliced Noxo1 isoforms. *Free Radic Biol Med* 42: 180–190, 2007.
47. Van der Perren A, Toelen J, Carlon M, Van den Haute C, Coun F, Heeman B, Reumers V, Vandenberghe LH, Wilson JM, Debyser Z, and Baekelandt V. Efficient and stable transduction of dopaminergic neurons in rat substantia nigra by rAAV 2/1, 2/2, 2/5, 2/6.2, 2/7, 2/8 and 2/9. *Gene Ther* 18: 517–527, 2011.
47a. West MJ, and Gundersen HJ. Unbiased stereological estimation of the number of neurons in the human hippocampus. *J Comp Neurol* 296: 1–22, 1990.
48. Wosniak JJ, Santos CX, Kowaltowski AJ, and Laurindo F. Cross-talk between mitochondria and NADPH oxidase: Effects of mild mitochondrial dysfunction on angiotensin II mediated increase in Nox isoform expression and activity in vascular smooth muscle cells. *Antioxid Redox Signal* 11: 1265–1278, 2009.
49. Wu DC, Teismann P, Tieu K, Vila M, Jackson-Lewis V, Ischiropoulos H, and Przedborski S. NADPH oxidase mediates oxidative stress in the 1-methyl-4-phenyl-1,2,3,6-tetrahydropyridine model of Parkinson's disease. *Proc Natl Acad Sci USA* 100: 6145–6150, 2003.
50. Zekry D, Epperson TK, and Krause KH. A role for NOX NADPH oxidases in Alzheimer's disease and other types of dementia? *IUBMB Life* 55: 307–313, 2003.

Address correspondence to:
Dr. Yoon-Seong Kim, M.D.
Burnett School of Biomedical Sciences
College of Medicine
University of Central Florida
6900 Lake Nona Blvd
Orlando, FL 32827

E-mail: yskim@mail.ucf.edu

Date of first submission to ARS Central, February 23, 2011; date of final revised submission, November 17, 2011; date of acceptance, November 18, 2011.

Abbreviations Used

AAV2 = adeno-associated virus serotype 2
AD = Alzheimer's disease
CNS = central nervous system
GFP = green fluorescence protein
LDH = lactate dehydrogenase
MPTP = 1-methyl-4-phenyl-1,2,3,6-tetrahydropyridine
NBT = nitroblue tetrazolium
NOX = NADPH oxidase
Noxa1 = Nox activator 1
Noxo1 = Nox organizer 1
6-OHDA = 6-hydroxydopamine
8-oxo-dG = 7,8-dihydro-8-oxo-deoxyguanine
PAK1 = p21-activated protein kinase 1
PBD = p21-binding domain
PD = Parkinson's disease
ROS = reactive oxygen species
SN = substantia nigra
SNpc = substantia nigra pars compacta
TH = tyrosine hydroxylase